International Journal of Control and Automation
Vol. 9, No. 5 (2016), pp. 55-66
http://dx.doi.org/10.14257/ijca.2016.9.5.06

Experimental Study on the Infrared Radiation Characteristics of the Diesel Engine Exhaust Plume by Infrared Imaging

Jia-feng Xu[1, a], Yang Du[1, b, *], Wei-dong Shen[2], Si-hong Song[2], Pei-li Zhang[1], Sheng-chun Wang[2]

[1] *Department of Petroleum Supply Engineering, Logistical Engineering University, Chongqing 401311, P. R. China*
[2] *Key Laboratory of Special Power Supply, Chongqing Communication Institute, Chongqing 400035, P.R. China*
[a]*jiafengxu518@163.com*, [b]*duyang58@163.com, * Corresponding Author*

Abstract

The variation ranges of species concentration, temperature and particle concentration of exhaust plume of the diesel engine with different load rate were tested in this article. Based on prototype experiment, the simulated generator and experimental platform of exhaust plume were built, and the effects of temperature, CO2, vapor and carbon soot on the infrared radiation characteristics of the exhaust plume were experimentally studied by infrared imaging. Experimental results showed that the temperature of the exhaust plume was the most important influencing factor for the infrared radiation characteristics, and the CO2 and carbon soot were also important influence factors too. However, the effects of the vapor could be neglected because of the slight influence on the infrared radiation characteristics of the exhaust plume.

Keywords: *Diesel engine exhaust plume; Infrared image; Infrared radiation characteristics; Species concentration*

1. Introduction

Due to the higher efficiency, fuel economy and reliability, diesel engine has been widely used as a main motive power in ground weapons [1]. The heat that exhaust plume took away are 35%-40% of the heat released in fuel combustion [2], and the exhaust plume contains large quantities of selective radiation gaseous species, such as CO_2, H_2O, *etc.*, and high temperature and emissivity carbon soot particles. These soot particles emissions of the diesel engines are usually 30 to 80 times of gasoline engine [3], so the diesel engines exhaust plume are main infrared radiation source [4]. Advanced infrared imaging technology widely used in military fields brings great detection and attack threats to the weapon which use diesel engines as motive powers [5].

Study on engine exhaust plume infrared radiation characteristic of rocket, aircraft, helicopter, artillery are very common in the reported literatures. Nam *et al* [6] devised an infrared radiation modeling of NO, OH, CO, H_2O, and CO_2 for emissivity prediction at high temperature. Avital *et al* [7] experimentally and computationally studied infrared radiation of rocket exhaust plumes. Snaza *et al* [8] modeled and investigated the effects of solid rocket motor propellant composition on plume infrared signature, considering that Al_2O_3 particles are main infrared radiation source of solid rocket exhaust plumes. Li *et al* [9] experimentally studied an aero-engine plume infrared characteristic under the condition of ground engine testing in afterburning and non-afterburning mode with infrared thermograph. Morris *et al* [10] experimentally studied of uncertainties in infrared camera measurements of a turbofan engine plume in an altitude test cell. Agboola *et al* [11]

ISSN: 2005-4297 IJCA

experimentally investigated nine different nozzle-mixing structure jets plume infrared radiation characteristics with infrared thermograph, considering that CO_2 is the main infrared radiation source of turbofan engine exhaust plumes. Pan *et al* [12, 13] numerically simulated temperature field, flow field and infrared radiation signature of the helicopter exhaust plume. Steward *et al* [14] experimentally investigated midwave infrared muzzle flash spectra from unsuppressed and flash-suppressed 152 mm howitzer. Andersson *et al* [15] and Bourayou *et al* [16] experimentally studied particles and gas radiation of flame with Fourier transform infrared (FTIR) spectrometer, considering that a large fraction of the radiation in these flames is emitted by particles. Although there are many differences between above research objects and diesel engine exhaust plume in concentration of exhaust species, temperature range, the results and methods of above researches can be referenced.

However, there are only a few studies focus on the infrared radiation characteristics of diesel engine exhaust plume at relatively low temperature. Zheng *et al* [17] established the numerical calculation model of flow field for tank plume and simulated the radiance and thermal image with C-G approximate model of channel bands, but the influence of carbon soot to plume was not considered. It can be seen from the literatures about infrared radiation characteristic of the diesel engine exhaust plume that most researches are numerical simulations and lack of systematic experimental study.

2. Experimental Set-Up and Methodology

2.1. Experimental Set-Up.

The experimental system of the diesel engine exhaust plume model and the infrared radiation characteristics test was shown in Figure 1, which was composed of the Lombardini LDW2204 diesel engine, hot jet producing system, exhaust species and carbon soot mixing system and test system. The prototype experiment and simulation experiment used the same test system and conditions.

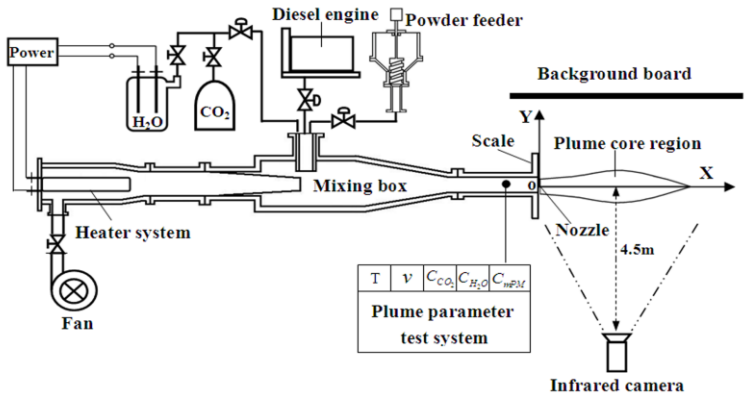

Figure 1. Schematic Diagram of the Diesel Engine Exhaust Plume Model and the Infrared Radiation Characteristics Test System

The exhaust species and carbon soot mixing system was consisted of CO_2 high-pressure bottle, electrical vapor generator, carbon soot supply equipment and mixing box. The CO_2 flowed into mixed box after being decompressed by decompress valve. The vapor flux was controlled by adjusting the voltage of generator and flux valve. The vertical helix carbon soot supply equipment was composed of speed governing electromotor, screw and power box. The quantity of

carbon soot supply was controlled by adjusting the rotate speed of electromotor. The carbon soot of diesel engine was composed of 0.1-10 μm carbon particle group, the carbon soot particle with 1 μm average diameter was used in the paper.

The infrared image of exhaust plume was tested by 3-5μm infrared radiation camera (Nikon LAIRD S270). In order to analyze expediently, the coordinate setup was shown in Figure1, in which the central axial direction of caudal nozzle was set as x axis, and the infrared image apparatus was mounted at 4.5m perpendicular distance of x axis to insure the whole exhaust plume was in the observational field of infrared image apparatus. The black woody board was used as shield background board to shield the infrared radiation effect of environment.

2.2. Methodology

The water cool diesel engine (LOMBARDINI LDW2204, rated power 32kw, rated rotate speed 3000 r/min) was used as study object in the paper. The parameters and infrared imaging of exhaust with different load rate were tested experimentally. The test results of exhaust parameters were shown in Table 1.

Table1. The Test Results of the Diesel Engine Exhaust Parameters

Load Rate (%)	T (k)	v (m/s)	C_{mPM} (mg/m^3)	C_{CO_2} (%vol)	C_{O_2} (%vol)	C_{CO} (%vol)	C_{HC} (10^{-6}vol)	C_{NO_x} (10^{-6}vol)	C_{H_2O} (%vol)
0	410.5	20.15	13.8	2.0	18.4	0.04	0	50	2.2
10	414.3	21.20	14.8	2.2	17.6	0.06	7	85	2.4
20	424.5	21.40	17.4	2.5	17.7	0.05	13	94	2.7
30	444.1	21.40	22.4	3.0	17.4	0.04	9	120	3.3
40	457.6	22.25	27.2	3.3	17.4	0.04	6	170	3.6
50	472.1	22.40	34.2	3.8	17.3	0.04	4	186	4.2
60	488.2	22.40	42.9	4.9	16.8	0.04	3	237	5.4
70	509.4	23.36	51.1	5.2	16.4	0.04	2	249	5.7
80	518.8	23.06	64.0	5.5	15.5	0.04	2	310	6.0
90	534.1	23.80	76.9	6.4	14.6	0.04	2	317	7.1
100	551.8	23.95	102.8	7.1	14.5	0.04	4	345	7.8

Table 2. The Single-Factor Simulation Experimental Scheme

Project	$T(K)$	$C_{mPM}(mg/m^3)$	$C_{CO_2}(\%vol)$	$C_{H_2O}(\%vol)$
1	343-573	102.8	0	0
2	473	0	0-8	0
3	473	0	0	0-8
4	473	0-110	0	0

It was found the experimental temperature variation range of diesel engine exhaust is close to that in Ref. 24. The exhaust species with radiant capability are mainly CO_2, H_2O, CO, HC, NO_x, but the effects of the CO, HC, NO_x on infrared radiation of exhaust plume can be neglected because their maximal concentration is not more than 5‰ of CO_2, H_2O volume concentration. The species concentration of CO_2, H_2O, carbon soot concentration and temperature could be looked as main four influencing factors on infrared radiation of exhaust plume in the paper. The experimental system as shown in Figure 1 was built, and the single-factor simulation experimental scheme was shown in Table 2. The variation ranges of the four main factors in simulation experiment were set on the base of the prototype experimental results. The effects of the four main factors in the tested value range on infrared radiation of exhaust plume were studied with the constant $v = 22m/s$.

2.3. Data Reduction

The tested infrared image shown in Figure 2 was study by being looked as surface object. The geometrical shape and infrared radiation characteristics of the object were analyzed in the paper. The infrared image of exhaust plume was analyzed and extracted data by the analysis software of the 3-5μm infrared radiation camera (Type Nikon LAIRD S270). The length L and area S of the core region of the exhaust plume could be calculated as follows:

$$L = \frac{L_S}{L_{SI}} L_{PI} \tag{1}$$

$$S = \frac{S_S}{S_{SI}} S_{PI} \tag{2}$$

Where L_S the length of the scale, and the scale is is 14.5 cm of the diameter of the flange. L_{SI} and L_{PI} are the imaging length of the scale and the exhaust plume, respectively. S_S is the $13.05\,cm^2$ of the radial section area of the scale. S_{SI} and S_{PI} are the imaging area of the scale and the exhaust plume, respectively.

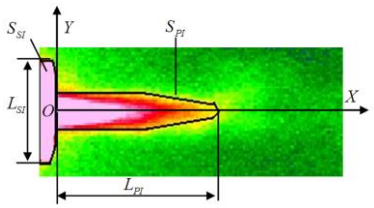

Figure 2. Geometric Characteristics of the Exhaust Plume and Scale in the Infrared Image

The infrared radiation parameters of the surface object include mainly the axial radiation temperature of exhaust plume, the average radiation temperature in S_{PI} area, the radiation exitance and the radiation flux. The radiation temperature and the average radiation temperature of the point, line or surface in the infrared image could be obtained by the FAI-Analyzer software. The follows can be achieved by the Stefan-Boltzmann law:

$$M_e = \varepsilon \sigma_b T^4 = \sigma_b T_R{}^4 \tag{3}$$

Where M_e is the radiation exitance, $\sigma_b = 5.67 \times 10^{-8} W/(m^2.k^4)$ is the radiation constant of black body, T is the thermodynamic temperature, T_R is the radiation temperature, ε is the emissivity.

The radiation exitance can be calculated by known radiation temperature, so the radiation flux can be obtained as:

$$\Phi_e = M_e S \tag{4}$$

3. Results and Discussion

3.1. Effects of the Load Rate on the Infrared Radiation Characteristics

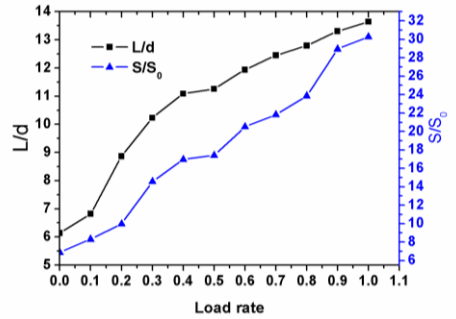

Figure 3a. Effects of the Load Rate on the Length the Area of the Exhaust Plume Core Region

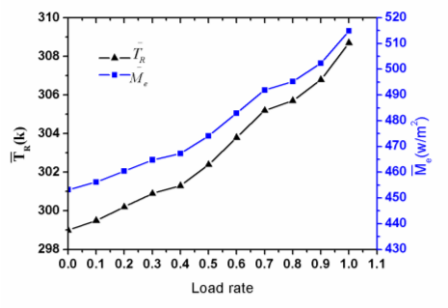

Figure 3b. Effects of the Load Rate on the $\bar{T}_R$ And $\bar{M}_e$ of the Exhaust Plume Core Region

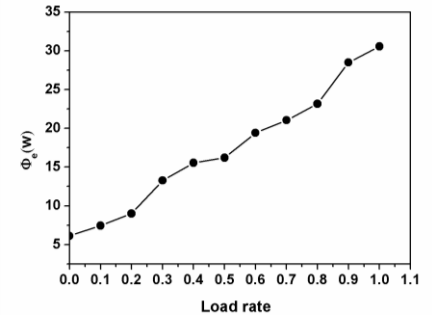

Figure 3c. Effects of the Load Rate on the Φ_e of the Exhaust Plume Core Region

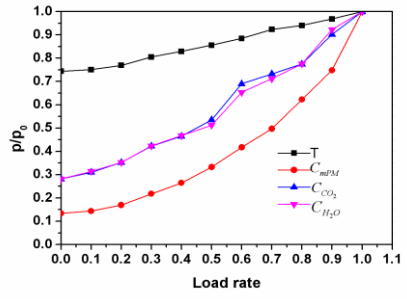

Figure 3d. Effects of the Load Rate on the Main Parameters of the Exhaust Plume

The effects of load rate on infrared radiation characteristics of the plume core region was investigated by prototype experiment, as shown in Figure 3a-3c. The dimensionless load rate is the ratio of the load to the rated load. The shape size of core region and infrared radiation energy of exhaust plume increase with increasing load rate quickly. The length and the area of the core region with rated load are 2.2 and 4.4 times that with null load, respectively. The $\bar{T}_R$ and $\bar{M}_e$ with rated load are 10K and 61.7 w/m^2 higher than that with null load, respectively. The variation of the radiation power of core region is brought by the area and radiation temperature. The Φ_e with rated load is 5 times that with null load. Because the amount of the diesel oil ejected into cylinder increases continually with increasing the load, the temperature, radiant gas and particle material of the exhaust plume increase continually. Figure3d indicates the variation of exhaust temperature, particle concentration and volume concentration of CO_2, H_2O with load rate. The four factors increase with load rate, specially, the particle concentration improves rapidly. Furthermore, the shape size of core region and infrared radiation energy of exhaust plume increase quickly with increasing load rate. Because it can't be confirmed which factor is the main influencing factor of infrared radiation characteristic of the core region, the individual experimental study of each factor needs to be performed.

3.2. Effects of the Temperature on the Infrared Radiation Characteristics

Figure 4a-4d show the effects of the temperature on infrared radiation characteristics with the project 1 in the table 2 and $C_{mPM}=102.8mg/m^3$. Figure 4a shows the infrared image of exhaust plume with different temperature. As shown in Figure 4a, the infrared radiation characteristics is not obvious when T<373K. As shown in Figure 4a-4d, the shape size of core region and infrared radiation energy of exhaust plume increase with increasing temperature quickly. The length and area of the core region with $T=558K$ are 8.8 and 21.7 time that with $T=373K$, respectively. The $\bar{T}_R$ and $\bar{M}_e$ with $T=558K$ are 10K and 59.9 w/m^2 higher than that with $T=373K$, respectively. It is generally considered that the infrared stealth can be realized when the radiation temperature difference between the target and the background is controlled at $\pm 4K$ [18]. In this experiment, the average radiation temperature of the background is 289K, the radiation temperature difference between the plume and the background is less than 4K when T<373K. The Φ_e with $T=558K$ is 24.8 times that with $T=373K$ .The Φ_e increases rapidly when $T>533K$.

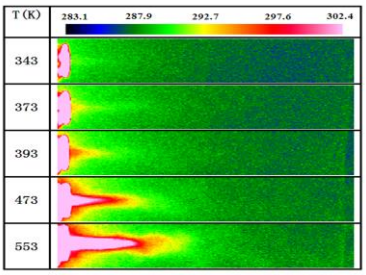

Figure 4a. The Infrared Image of the Exhaust Plume with Different Temperature

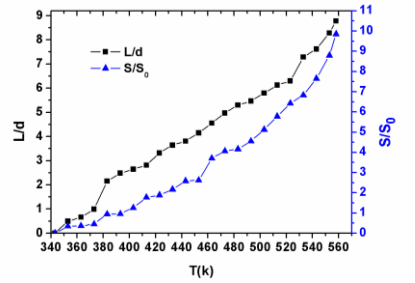

Figure 4b. Effects of the Temperature on the Length and the Area of the Exhaust Plume Core Region

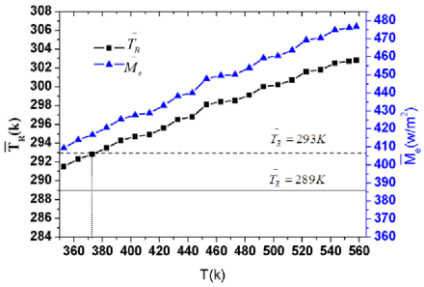

Figure 4c. Effects of the Temperature on the $\bar{T}_R$ and $\bar{M}_e$ of the Exhaust Plume Core Region

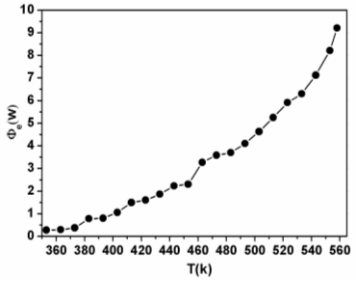

Figure 4d. Effects of the Temperature on the Φ_e of the Exhaust Plume Core Region

According to the radiation function of black body, the radiation exitance of different temperature object at 3-5 μm can be calculated as follows:

$$M_{b(3-5)}=M_b(F_{b(0-5)}-F_{b(0-3)})=M_bF_{b(3-5)} \quad (5)$$

The radiation function of black body ($F_{b(0-\lambda T)}$) is shown as Equation (6).

$$F_{b(0-\lambda T)} = \int_0^{\lambda T} \frac{C_1}{\sigma_b (\lambda T)^5 \left(\exp \frac{C_2}{\lambda T} - 1 \right)} d(\lambda T) = \int_0^{\lambda T} \frac{M_{b\lambda}}{\sigma_b T^5} d(\lambda T) \quad (6)$$

Where C_1, C_2 are constant, σ_b is the radiation constant of black body. According to Stefan-Boltzmann law, M_b is in direct proportion to T^4.On the other hand, the $F_{b(3-5)}$ increases with increasing the temperature. The calculated $F_{b(3-5)}$ at T=343-558K range is shown in Figure 5, and the $F_{b(3-5)}$ with $T = 558K$ is 4.2 times that with $T = 373K$. So the infrared radiation energy of the core region increases with increasing the temperature.

Figure 6 shows the distributing of tested physical and radiation temperature of the exhaust plume at $T = 473K$. Because the exhaust with high temperature has the heat exchange with environmental cool air by roll indraft and mixing, the temperature of the exhaust plume decreases along the X direction. The physical and radiation temperature of the exhaust plume go down to near 400K and environmental radiation temperature at $X = 5d$, respectively.

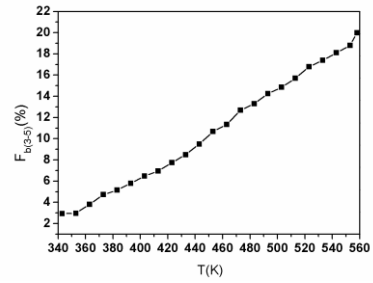

Figure 5. Variation of the Radiation Function of Black Body with Temperature

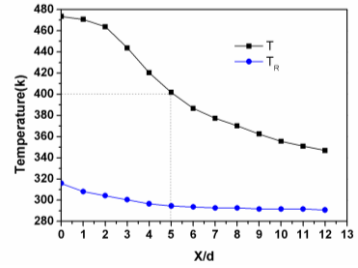

Figure 6. Axial Distribution of Tested Physical and Radiation Temperature of the Exhaust Plume At $T = 473K$ and $C_{mPM} = 102.8mg/m^3$

3.3. Effects of the CO2 Concentration on the Infrared Radiation Characteristics

Figure 7a-7c show the effects of the CO_2 concentration on infrared radiation characteristics with the project 2 in the table 2 and $T = 473K$. As shown in Figure 7a-7c, the shape size of core region and infrared radiation energy of exhaust plume increase with increasing the C_{co_2}. The Φ_e increase with increasing the C_{co_2}, and the Φ_e with $C_{co_2} = 8\%$ is the 3 times that with $C_{co_2} = 2\%$. Because the CO_2 is the typical radiant gas with frequency selecting characteristic, the C_{co_2} has the important effects on the infrared radiation characteristics of the exhaust plume.
According to Kirchhoff's law, the correlation of monochromatic radiance and monochromatic absorptivity can be written as:

$$\varepsilon_\lambda = \alpha_\lambda = 1 - e^{-K_{\lambda.CO_2} P_i s_{CO_2}} \quad (7)$$

Where $K_{\lambda.co_2}$ is monochromatic weaken coefficient, P_i is partial pressure of gas, s_{CO_2} is average travel of radial.

The absorbing spectrum in infrared wave band of CO_2 and vapor is equal to the

radiation spectrum. According to the absorbing spectrum in infrared wave band of CO_2 and vapor, it could be found that the infrared radiation of CO_2 exits in the 2.65-2.8 μm and 4.2 - 4.5 μm radiation band, and the 4.2 - 4.5 μm radiation band is the main strong radiation band for CO_2. The $K_{\lambda.co_2}$ and s_{CO_2} are constant because the temperature field, pressure field and flow field in the experiment are almost constant. Furthermore, because the partial pressure is in direct proportion to the C_{CO_2}, and according to Equation(6), the emissivity of plume increase with increasing C_{CO_2}, the infrared radiation size and energy of exhaust plume increase with increasing C_{CO_2}.

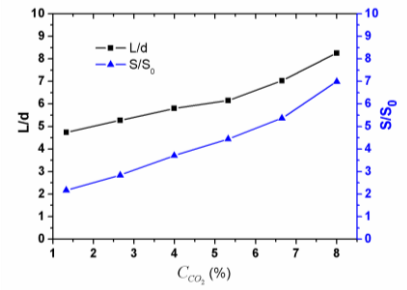

Figure7a. Effects of the CO_2 Concentration on the Length and the Area of the Exhaust Plume Core Region

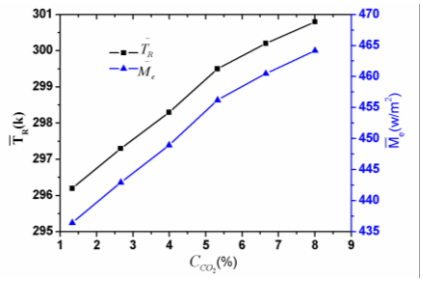

Figure 7b. Effects of the CO_2 Concentration on the $\bar{T}_R$ and $\bar{M}_e$ of the Exhaust Plume Core Region

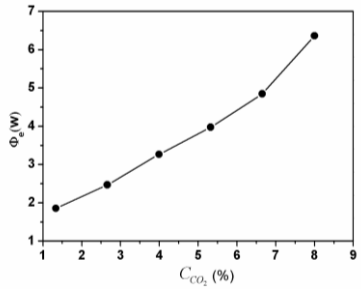

Figure 7c. Effects of the CO_2 Concentration on the Φ_e Of The Exhaust Plume Core Region

3.4. Effects of the Vapor Concentration on the Infrared Radiation Characteristics

Figure 8a-8c show the effects of the vapor concentration on infrared radiation characteristics with the project 3 in the table 2 and $T = 473K$. As shown in Figure 8a-8c, the shape size of core region and infrared radiation energy of exhaust plume increase slightly with increasing the C_{H_2O}. The $\bar{T}_R$ and $\bar{M}_e$ with $C_{H_2O} = 7.8\%$ are only 0.4k and 2.17 w/m^2 higher than that of $C_{H_2O} = 2.2\%$, respectively. The C_{H_2O} has slight effects on the infrared radiation characteristics of the exhaust plume, because the radiation power of the vapor at the 2.55-2.84 μm band is less than that of the CO_2 at the 4.2 - 4.5 μm band, and the radiation wave band of the vapor is not located in the 3-5 μm range, the C_{H_2O} is not the main factor on infrared radiation characteristics of the exhaust plume.

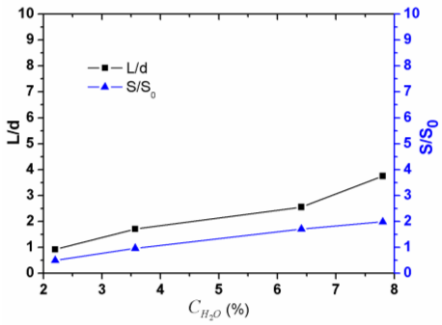

Figure 8a. Effects Of The Vapor Concentration On The Length And The Area Of The Exhaust Plume Core Region

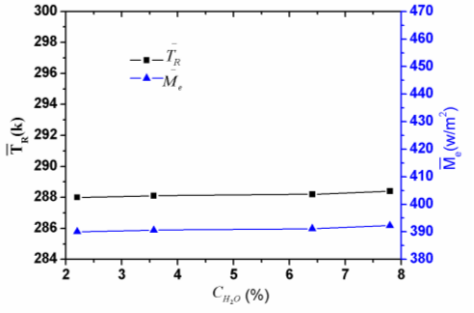

Figure 8b.Effects Of The Vapor Concentration On The $\bar{T}_R$ And $\bar{M}_e$ Of The Exhaust Plume Core Region

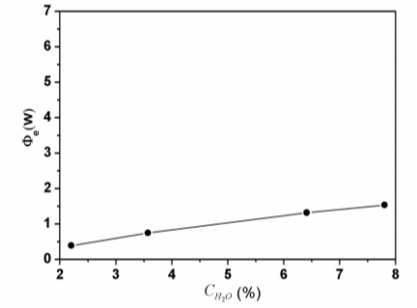

Figure 8c. Effects of the Vapor Concentration on the Φ_e of the Exhaust Plume Core Region

3.5 Effects of the Particle Concentration on the Infrared Radiation Characteristics

Figure 9a-9c show the effects of the particle concentration on infrared radiation characteristics with the project 4 in the table 2 and $T = 473K$. As shown in Figure 9a-9c the shape size of core region and infrared radiation energy of exhaust plume increase with increasing the C_{mPM} quickly. The $\bar{T}_R$ and $\bar{M}_e$ with $C_{mPM} = 102.8mg/m^3$ are 4.3k and 25.3 w/m^2 higher than that of $C_{mPM} = 13.8mg/m^3$, respectively. The Φ_e with $C_{PM} = 102.8mg/m^3$ is 6 times higher than that with $C_{PM} = 13.8mg/m^3$. The C_{mPM} has important effects on the infrared radiation characteristics of the exhaust plume.

Because carbon soot and participatory media in plume component particle radiation system, the correlation of monochromatic radiance and monochromatic absorptivity can be written as:

$$\varepsilon_\lambda = \alpha_\lambda = 1 - e^{-K_{\lambda.PM} s_{PM}} \tag{8}$$

Where $K_{\lambda.PM}$ is carbon soot monochromatic weaken coefficient, s_{PM} is average travel of exhaust plume radial. When $\lambda > 0.8\mu m$:

$$K_{\lambda.PM} = \frac{C_1 C_{mPM}}{\rho \lambda^{0.95}} \times 10^{-6} \tag{9}$$

Where C_1 is constant, ρ is the density of carbon soot, C_{mPM} is mass

concentration (mg/m3) of carbon soot. It can been seen that the emissivity of plume increase with increasing C_{mPM}, which lead to that the infrared radiation size and energy of exhaust plume increase with increasing C_{mPM}. As shown in Figure 10, the radiation temperature of exhaust plume along the middle line of X axis decrease rapidly with decreasing the particle concentration. Furthermore, the radiation temperature of exhaust plume at exit increases rapidly with increasing the concentration of the carbon soot.

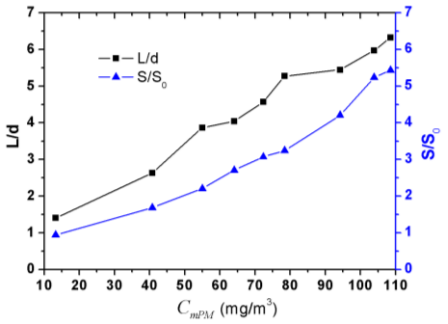

Figure9a. Effects of the C_{mPM} on the Length and the Area of the Exhaust Plume Core Region

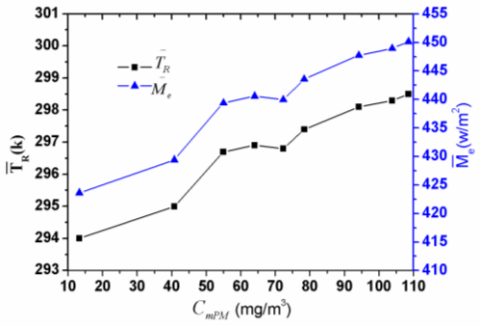

Figure 9b. Effects Of The C_{mPM} on the $\bar{T}_R$ And $\bar{M}_e$ of the Exhaust Plume Core Region

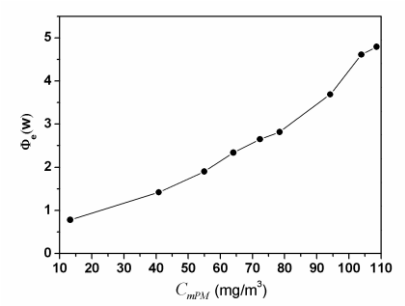

Figure 9c. Effects Of The C_{mPM} on the Φ_e of the Exhaust Plume Core Region

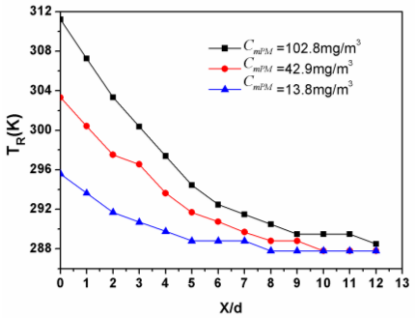

Figure 10. Axial Distribution of T_R of the Exhaust Plume with Different C_{mPM}

3.6. Sensitivity Analysis of Each Factor on the Infrared Radiation Characteristics

Figure 11 shows the effects of each factor on the infrared radiation flux of the exhaust plume. In order to facilitate comparative analysis, the abscissa were normalized and non-dimensionalized. As shown in Figure 11, the temperature is the most important parameter influencing the infrared radiation characteristics of the exhaust plume, and the radiation flux increase with increasing temperature rapidly. The CO_2 and carbon soot also influence the infrared radiation characteristics of the exhaust plume, the radiation flux increase with increasing C_{co_2} and C_{mPM}, and the $\overline{\Phi}_e$ of CO_2 are 1.02w higher than that of carbon soot. However, the vapor influences slightly the infrared radiation characteristics of the exhaust plume,the $\overline{\Phi}_e$ of vapor is not more than 26% and 35% of CO_2 and carbon soot, respectively. Therefore, the CO_2 and carbon soot is the most important gaseous and solid infrared source of diesel exhaust plume, respectively. Figure 12 and Figure 13 show the

infrared image and the radiation temperature distributing along middle line of the exhaust plume with different species and temperature of the exhaust plume, respectively. The same results from Figure 11 are also found from Figure 12 and Figure 13.

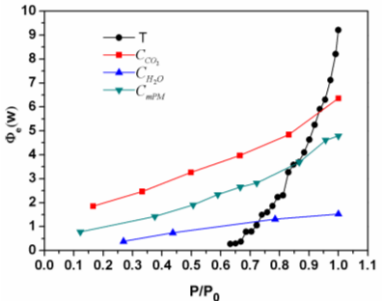

Figure 11. Effects of Each Factor on the Φ_e of the Exhaust Plume Core Region

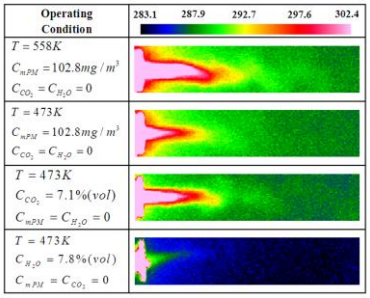

Figure 12. Infrared Image of Exhaust Plume with Different Parameters

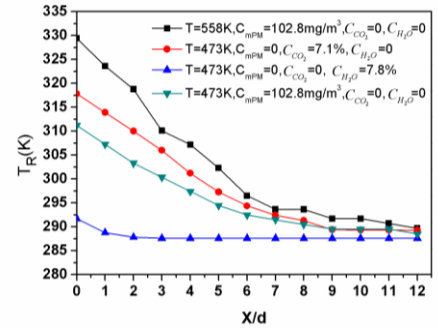

Figure 13. Axial Distribution of Radiation Temperature of the Exhaust Plume with Different Parameters

4. Conclusions

In this paper, the parameters and infrared images of the diesel engine exhaust were tested, and the four main factors influencing the infrared radiation characteristics of the exhaust plume were studied experimentally. The important conclusions can be concluded as follows:

(1) The load rate of the diesel engine influences greatly the infrared radiation characteristics of the exhaust plume. The shape size and the infrared radiation energy of the core region increase rapidly with increasing the load rate. Furthermore, the species concentration of exhaust and carbon soot particle increase with increasing the load rate.

(2) The temperature of the exhaust plume is the most important influencing factor for the infrared radiation characteristics. The infrared radiation capability increases rapidly with increasing the temperature. The infrared characteristic of the exhaust plume can be eliminated availably if the temperature of the exhaust plume dipped under 373 K.

(3) The CO_2 also influences greatly the infrared radiation characteristics of the exhaust plume. However, the vapor influences slightly the infrared radiation characteristics of the exhaust plume, and the effects of the vapor can be neglected.

(4) The carbon soot is an important factor influencing the infrared radiation characteristics of the exhaust plume. The infrared radiation capability increases with increasing the carbon soot concentration. The CO_2 and carbon soot is the most

important gaseous and solid infrared source of diesel exhaust plume. However, the influencing extent of carbon soot is less than that of CO_2 and more than that of vapor.

References

[1] R. Royo, M.A. Albertos-Arranz, J.A. Carcel-Cubas and J. Paya, "Thermographic study of the preheating plugs in diesel engines", Applied Thermal Engineering. vol.37, **(2012)**, pp.412-419.
[2] S.Y. Zhu, D.M. Wei, J.T. Yao and X.Q. Zhou, "Research on MBT and infrared irradiation characteristics with ground-object background, Infrared Technology", vol. 22, no. 5, **(2000)**, pp. 45-60.
[3] J. Liu, Z. Zhao and C.M. Xu, "Research progress in catalysts for removal of soot particulates from diesel engines", Chinese Journal of Catalysis, vol. 25, no. 8, **(2004)**, pp. 673-680.
[4] J.C. Li, C. Yang and H.F. Zheng, "Study on infrared suppressor ejected by armored vehicle exhaust, Journal of Sichuan Ordnance", vol. 32, No. 10, **(2011)**, pp. 70-73.
[5] S.Y. Zhu, D.M. Wei, X.Q. Zhou and J.T. Yao, "Study on the heat insulating techonology used in exhaust pipe of tank engine, ACTA Armamentarll the Volume of Tank Armored Vehicle and Engine, vol. 73, **(1999)**, pp. 1-14.
[6] H.J. Nam and O.J. Kwon, "Infrared radiation modeling of NO, OH, CO, H2O, and CO2 for emissivity/radiance prediction at high temperature", Infrared Physics & Technology, vol.67, **(2014)**, pp. 283-291.
[7] G. Avital, Y. Cohen, L. Gamss, Y. Kanelbaum and J. Macales, "Experimental and computational study of infrared emission from underexpanded rocket exhaust plumes", Journal of Thermophysics and Heat Transfer, vol.15, **(2001)**, no. 4, pp. 377-383.
[8] C. J. Snaza, "Investigation of the effects of solid rocket motor propellant composition on plume signature", M.S Thesis, Naval Postgraduate School, Monterey, California, USA, **(1994)**, pp.17-25.
[9] J.X. Li, Z.X. Tong, W.J. Liu, C.Z. Wang, Z.B. Zhang and Z.F. Zhuo, "Infrared radiation characteristic experiment and simulation of aeroengine", Infrared and Laser Engineering, vol. 42, no. 3, **(2013)**, pp. 449-555.
[10] T.A. Morris, M.A. Marciniak, G.C. Wollenweber and J.A., "Turk, Analysis of uncertainties in infrared camera measurements of a turbofan engine in an altitude test cell", Infrared Physics & Technology, vol.48, **(2006)**, pp. 130-153.
[11] F.A. Agboola and J. Bridges, "Measurements of infrared and acoustic source distributions in jet plumes, NASA/TM 2004-213042, Washington, USA, vol. 4, no. 2, **(201**3**)**.
[12] C.X. Pan, J.Z. Zhang and Y. Shan, "Effects of exhaust temperature on helicopter infrared signature", Applied Thermal Engineering, vol.51, **(2013)**, pp. 529-538.
[13] C.X. Pan, J.Z. Zhang and Y. Shan, "Modeling and analysis of helicopter thermal and infrared radiation", Chinese Journal of Aeronautics, vol.24, **(2011)**, pp. 558-567.
[14] B.J. Steward, G.P. Perram and K.C. Gross, "Modeling midwave infrared muzzle flash spectra from unsuppressed and flash-suppressed large caliber munitions", Infrared Physics & Technology, vol.55, **(2012)**, pp. 246-255.
[15] K. Andersson, R. Johansson, S. Hjartstam, F. Johnsson and B. Leckner, "Radiation intensity of lignite-fired oxy-fuel flames", Experimental Thermal and Fluid Science, vol.33, **(2008)**, pp. 67-76.
[16] R. Bourayou, R. Vaillon and J.F. Sacadura, "FTIR low resolution emission spectrometry of a laboratory-scale diffusion flame: experimental set-up", Experimental Thermal and Fluid Science, vol.26, **(2002)**, pp. 181-187.
[17] K.P. Zheng, X.P. Bi, X.H Huang and P.K. Wang, "Infrared radiation calculation and thermal image simulation of fume released from the tank", Laser & Infrared, vol.40, no.6, **(2010)**, pp. 613-616.
[18] J.K. Yi and K.J. Li, "Algorithm for thermal radiation characteristics of smoke from exhaust pipes of tanks", Journal of Beijing Institute of Technology, vol.18, no.2, **(1998)**, pp. 145-149.

